

Supplementary Material

New boron-based coumarin fluorophores for bioimaging applications

Anita Marfavi^{A,B}, Jia Hao Yeo^A, Kathryn G. Leslie^A, Elizabeth J. New^{A,B,C} and Louis M. Rendina^{A,B,*}

^ASchool of Chemistry, The University of Sydney, Sydney, NSW 2006, Australia

^BThe University of Sydney Nano Institute, Sydney, NSW 2006, Australia

^CAustralian Research Council Centre of Excellence for Innovations in Peptide and Protein Science, The University of Sydney, Sydney, NSW 2006, Australia

*Correspondence to: Email: louis.rendina@sydney.edu.au

Confocal Microscopy

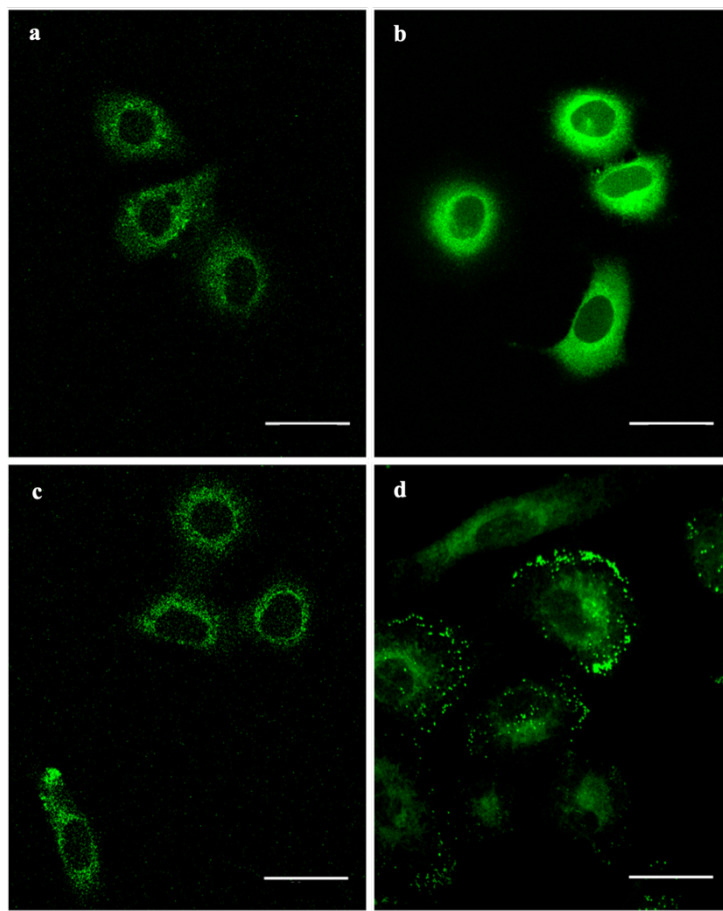


Figure S1: Confocal microscopy images of A549 cells treated with (a) **HCoBA** (10 μM , 20 min), (b) **HCpBA** (10 μM , 20 min), (c) **ICPh** (10 μM , 20 min), and (d) **ICCb** (10 μM , 20 min), showing coumarin fluorescence ($\lambda_{\text{ex}} = 458 \text{ nm}$, $\lambda_{\text{em}} = 468\text{-}568 \text{ nm}$). Scale bar represents 30 μm .

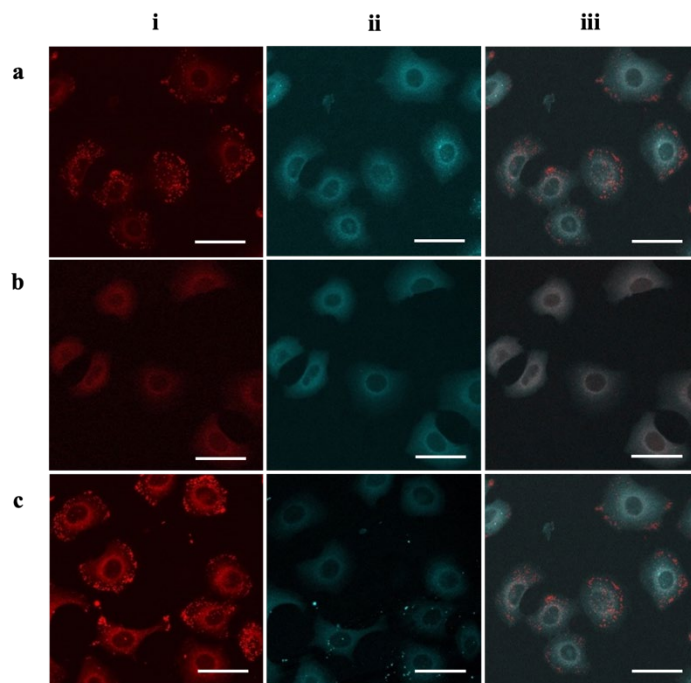


Figure S2. Confocal microscopy images of A549 cells treated with Nile Red (50 μ M, 20 min) and (a) **HCoBA** (10 μ M, 20 min), (b) **HCmBA** (10 μ M, 20 min), or (c) **HCpBA** (10 μ M, 20 min), showing (i) Nile Red fluorescence ($\lambda_{\text{ex}} = 561$ nm, $\lambda_{\text{em}} = 571 - 700$ nm), (ii) coumarin fluorescence ($\lambda_{\text{ex}} = 458$ nm, $\lambda_{\text{em}} = 468 - 568$ nm), and (iii) overlay of (i) and (ii). Pearson's correlation coefficient for treatment with Nile Red are: **HCoBA** ($R = 0.27 \pm 0.03$), **HCmBA** ($R = 0.34 \pm 0.04$), and **HCpBA** ($R = 0.40 \pm 0.03$). Scale bar represents 30 μ m.

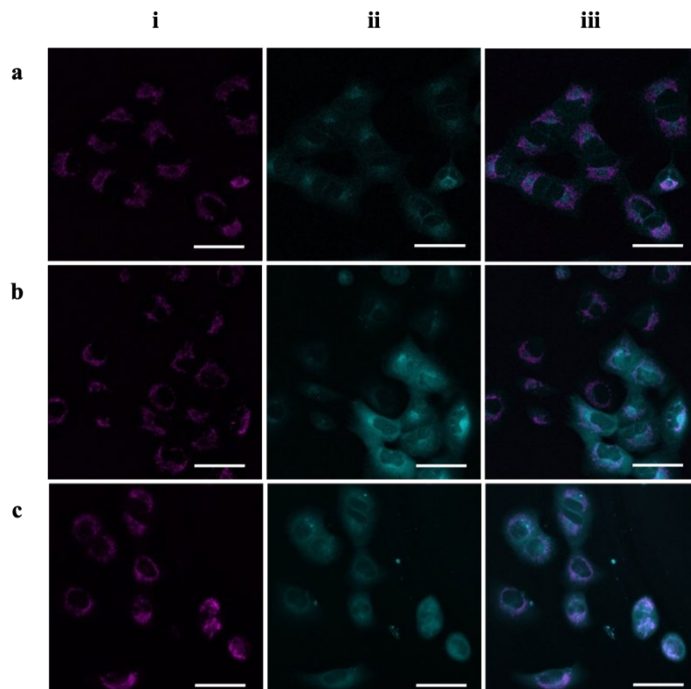


Figure S3. Confocal microscopy images of A549 cells treated with MitoTracker Red CMXRos (100 nM, 20 min) and (a) **HCoBA** (10 μ M, 20 min), (b) **HCmBA** (10 μ M, 20 min), or (c) **HCpBA** (10 μ M, 20 min), showing (i) MitoTracker Red CMXRos fluorescence ($\lambda_{\text{ex}} = 561$ nm, $\lambda_{\text{em}} = 570 - 767$ nm), (ii) coumarin fluorescence ($\lambda_{\text{ex}} = 458$ nm, $\lambda_{\text{em}} = 468 - 568$ nm), and (iii) overlay of (i) and (ii). Pearson's correlation coefficient for treatment with MitoTracker Red CMXRos are: **HCoBA** ($R = 0.22$), **HCmBA** ($R = 0.17$), and **HCpBA** ($R = 0.55$). Scale bar represents 40 μ m.

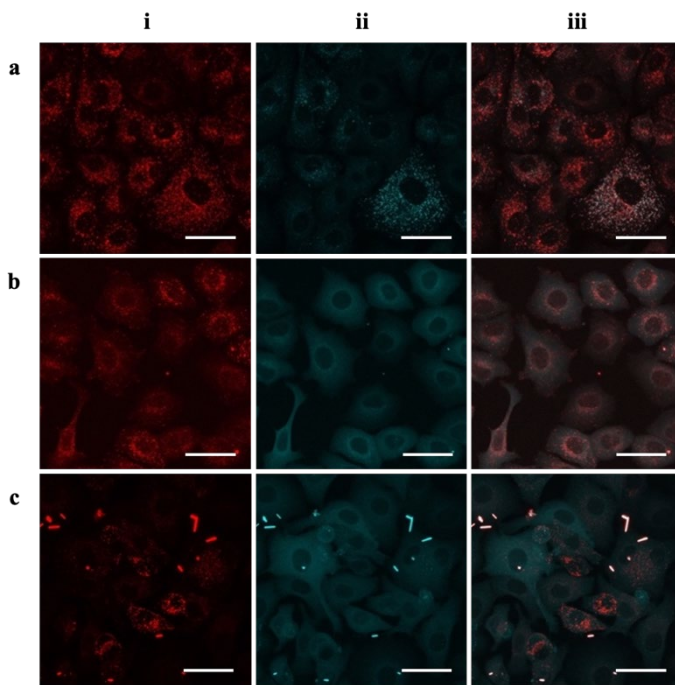


Figure S4. Confocal microscopy images of A549 cells treated with Lysotracker Red DND-99 (50 nM, 20 min) and (a) **HCoBA** (10 μ M, 20 min), (b) **HCmBA** (10 μ M, 20 min), or (c) **HCpBA** (10 μ M, 20 min), showing (i) Lysotracker Red DND-99 fluorescence ($\lambda_{\text{ex}} = 561$ nm, $\lambda_{\text{em}} = 568 - 701$ nm), (ii) coumarin fluorescence ($\lambda_{\text{ex}} = 458$ nm, $\lambda_{\text{em}} = 468 - 568$ nm), and (iii) overlay of (i) and (ii). NB: Row c shows some evidence of probe precipitation. Pearson's correlation coefficient for treatment with Lysotracker Red DND-99 are: **HCoBA** ($R = 0.30 \pm 0.06$), **HCmBA** ($R = 0.33 \pm 0.03$), and **HCpBA** ($R = 0.39 \pm 0.04$). Scale bar represents 40 μ m.

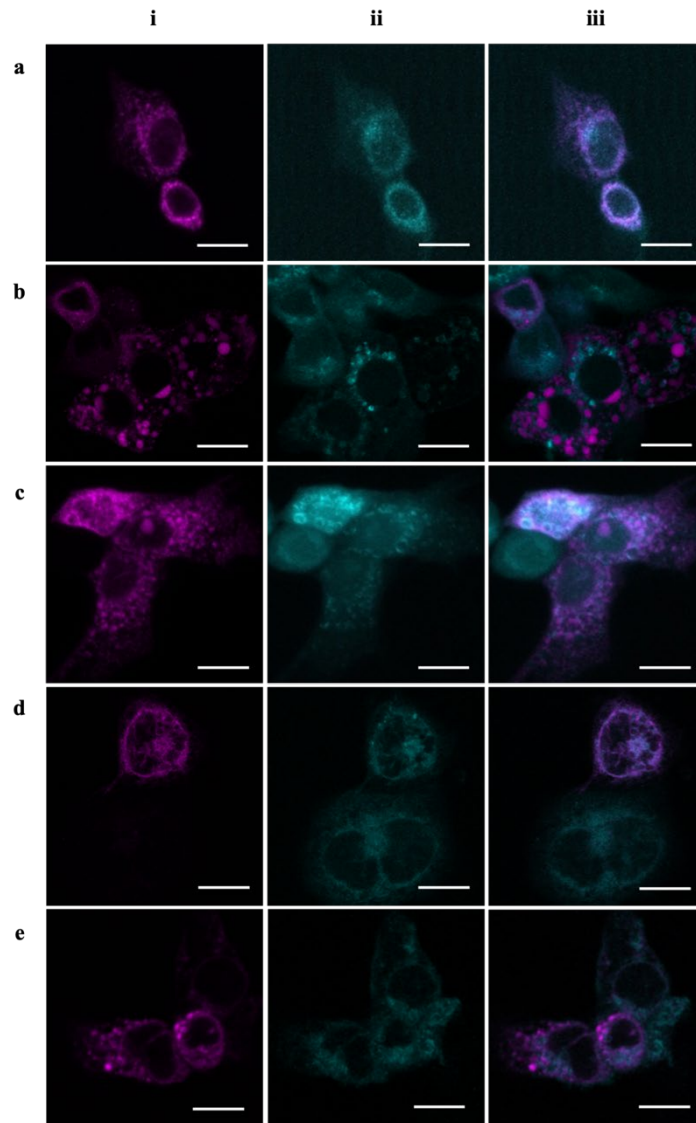


Figure S5: Confocal microscopy images of DLD-1 cells transfected with mCherry-ER and treated with (a) **HCoBA** (10 μ M, 20 min), (b) **HCmBA** (10 μ M, 20 min), (c) **HCpBA** (10 μ M, 20 min), (d) **HCCb** (10 μ M, 20 min), or (e) **ICCb** (10 μ M, 20 min), showing (i) mCherry-ER fluorescence ($\lambda_{\text{ex}} = 561$ nm, $\lambda_{\text{em}} = 581 - 653$ nm), (ii) coumarin fluorescence ($\lambda_{\text{ex}} = 458$ nm, $\lambda_{\text{em}} = 468 - 568$ nm), and (iii) overlay of (i) and (ii). Pearson's correlation coefficients observed: **HCoBA** ($R = 0.67 \pm 0.03$), **HCmBA** (0.60 ± 0.07), **HCpBA** ($R = 0.73 \pm 0.07$), **HCCb** ($R = 0.47 \pm 0.03$), and **ICCb** ($R = 0.41 \pm 0.05$). Scale bar represents 20 μ m.

Fluorescence Spectroscopy

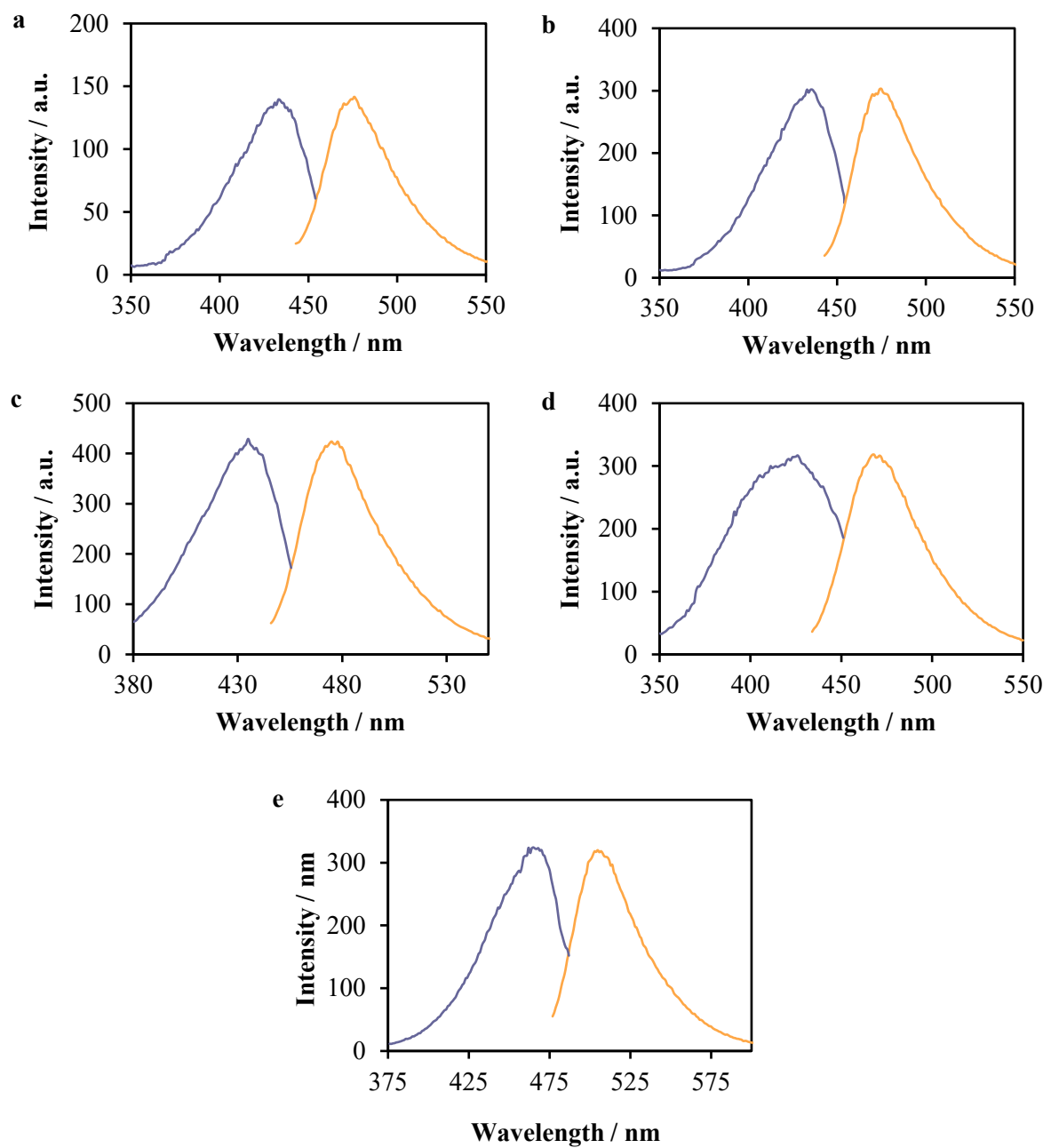


Figure S6: Excitation (blue) and emission (orange) spectra for the boron-based coumarins: (a) **HCoBA** ($1 \mu\text{M}$, $\lambda_{\text{ex}} = 433 \text{ nm}$), (b) **HCmBA** ($1 \mu\text{M}$, $\lambda_{\text{ex}} = 433 \text{ nm}$), (c) **HCpBA** ($1 \mu\text{M}$, $\lambda_{\text{ex}} = 435 \text{ nm}$), (d) **HCCb** ($1 \mu\text{M}$, $\lambda_{\text{ex}} = 425 \text{ nm}$), (e) **ICCb** ($1 \mu\text{M}$, $\lambda_{\text{ex}} = 465 \text{ nm}$).

NMR and MS Spectra of Novel Compounds

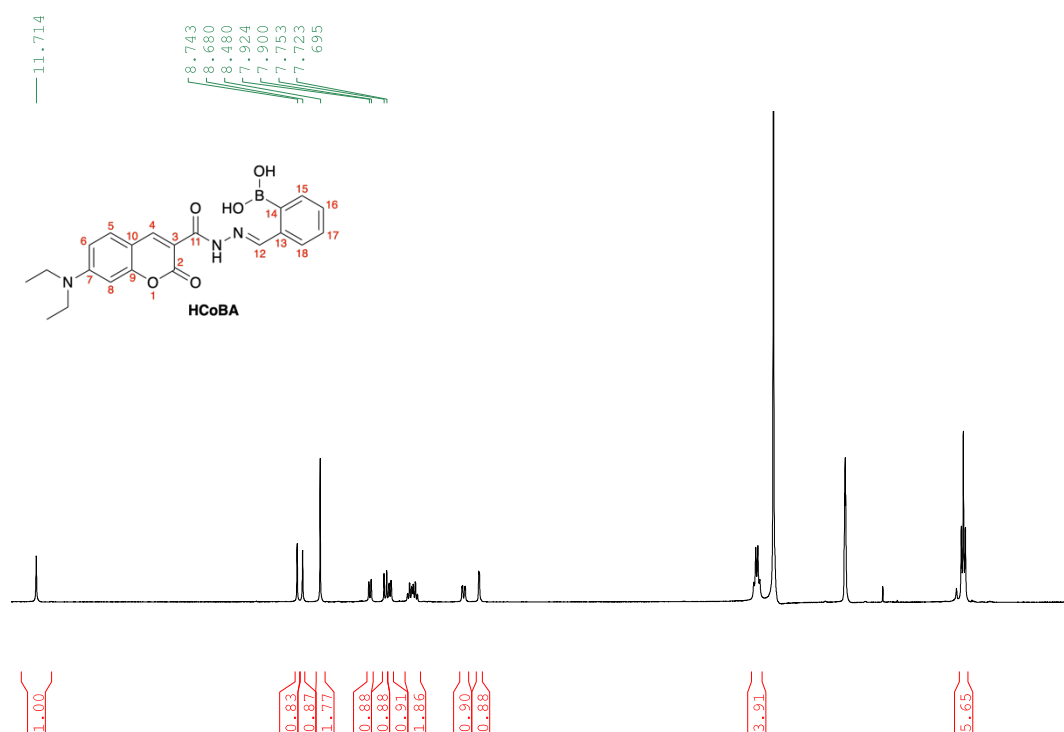


Figure S7.1: ¹H NMR spectrum of HCoBA in DMSO-*d*₆.

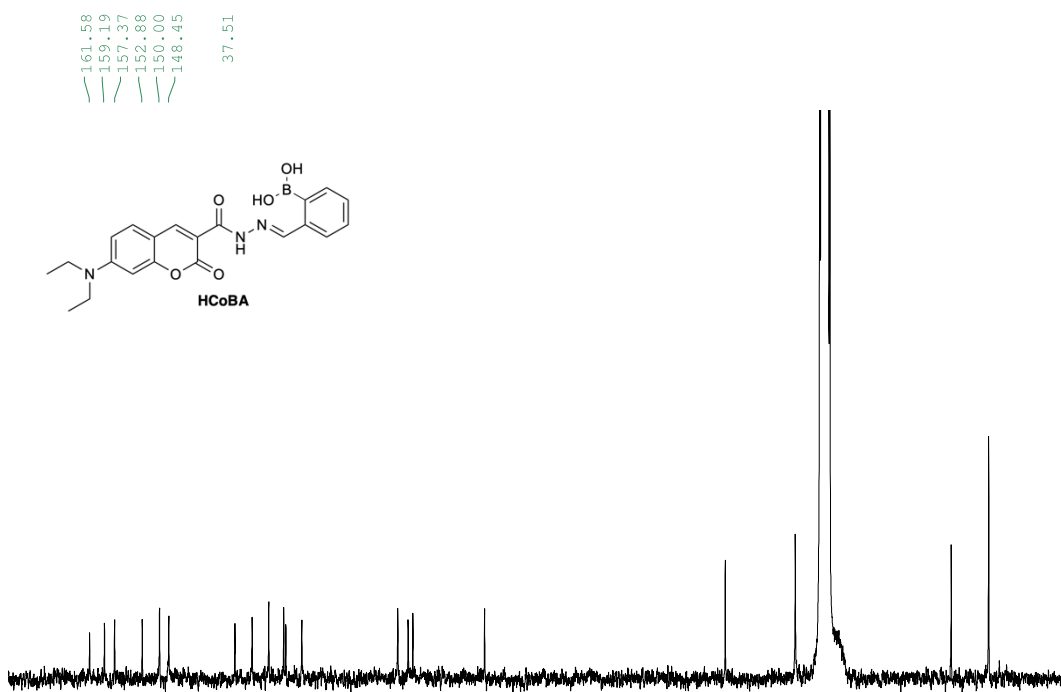


Figure S7.2: ¹³C NMR spectrum of HCoBA in DMSO-*d*₆.

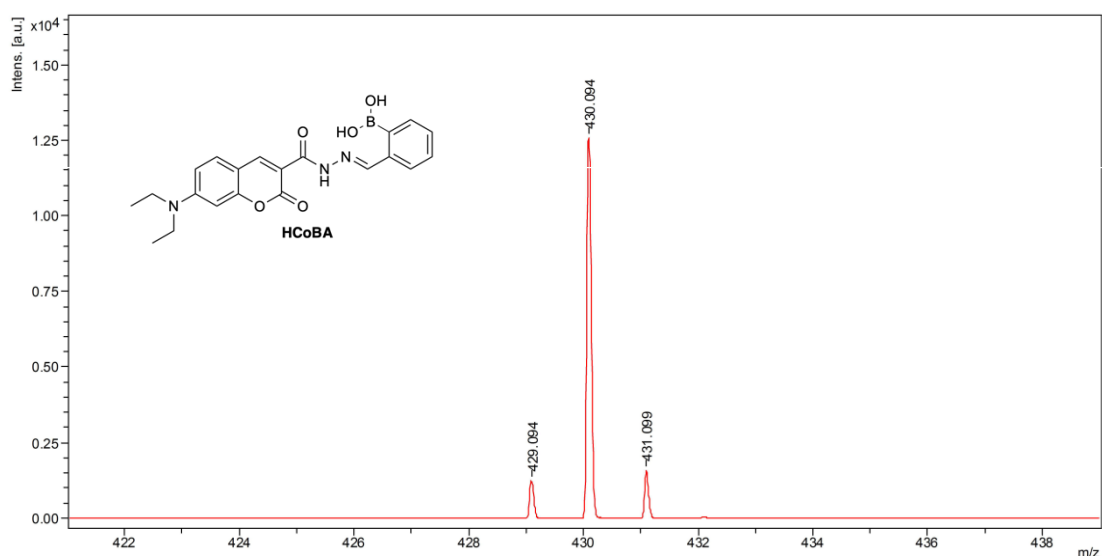


Figure S7.3: MALDI-TOF mass spectrum of HCoBA.

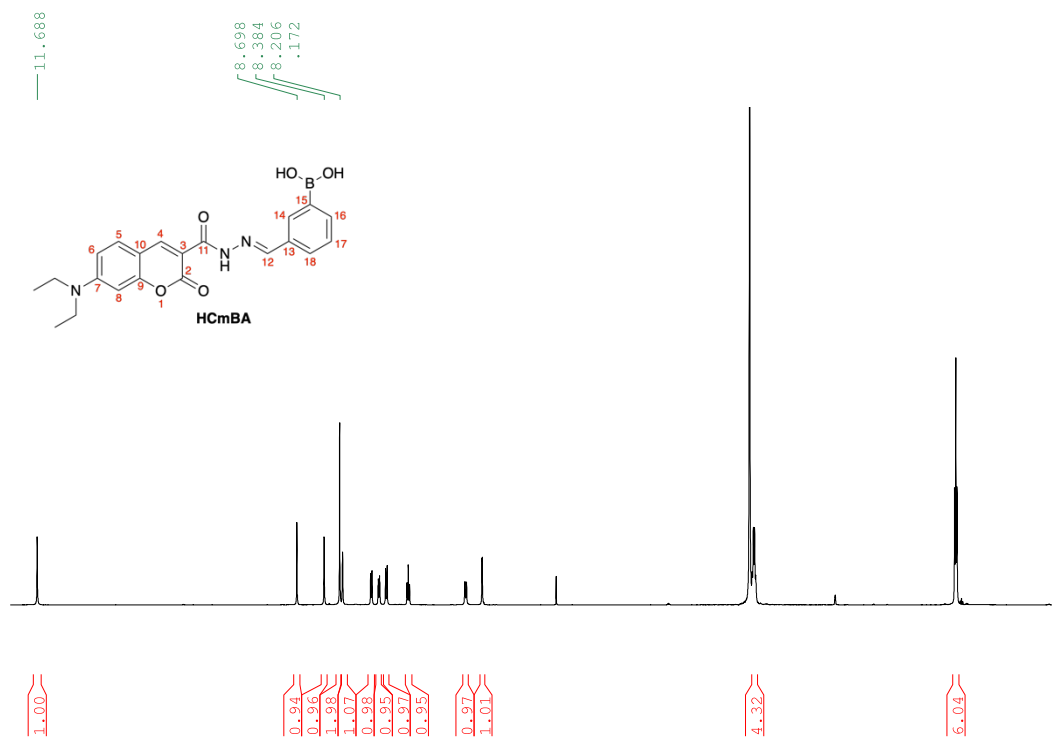


Figure S8.1: ^1H NMR spectrum of HCmBA in $\text{DMSO}-d_6$.

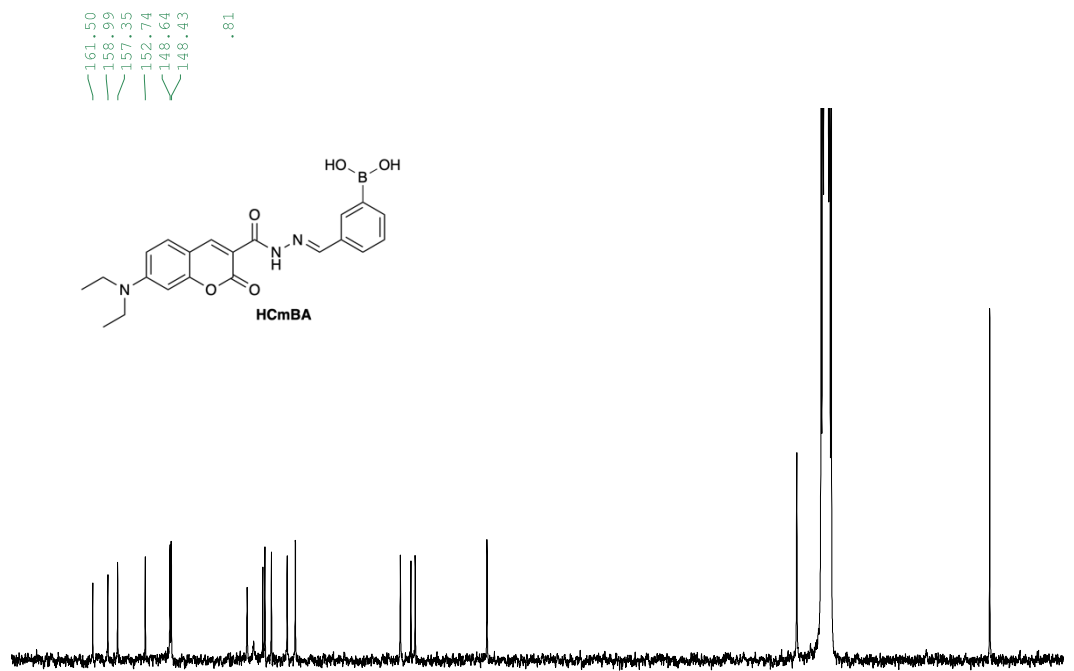


Figure S8.2: ^{13}C NMR spectrum of **HCmBA** in $\text{DMSO}-d_6$.

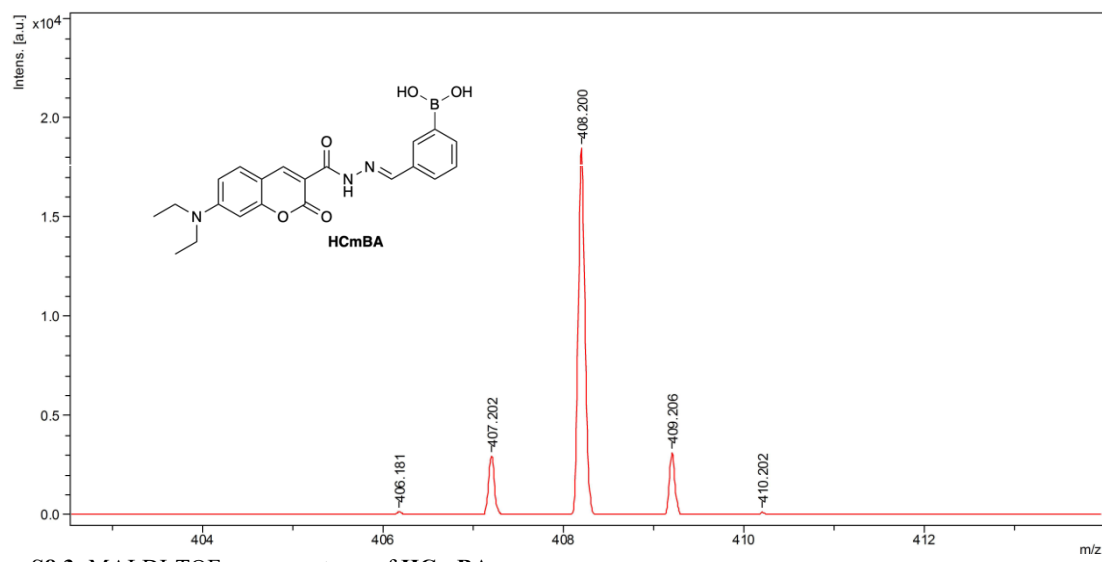


Figure S8.3: MALDI-TOF mass spectrum of **HCmBA**.

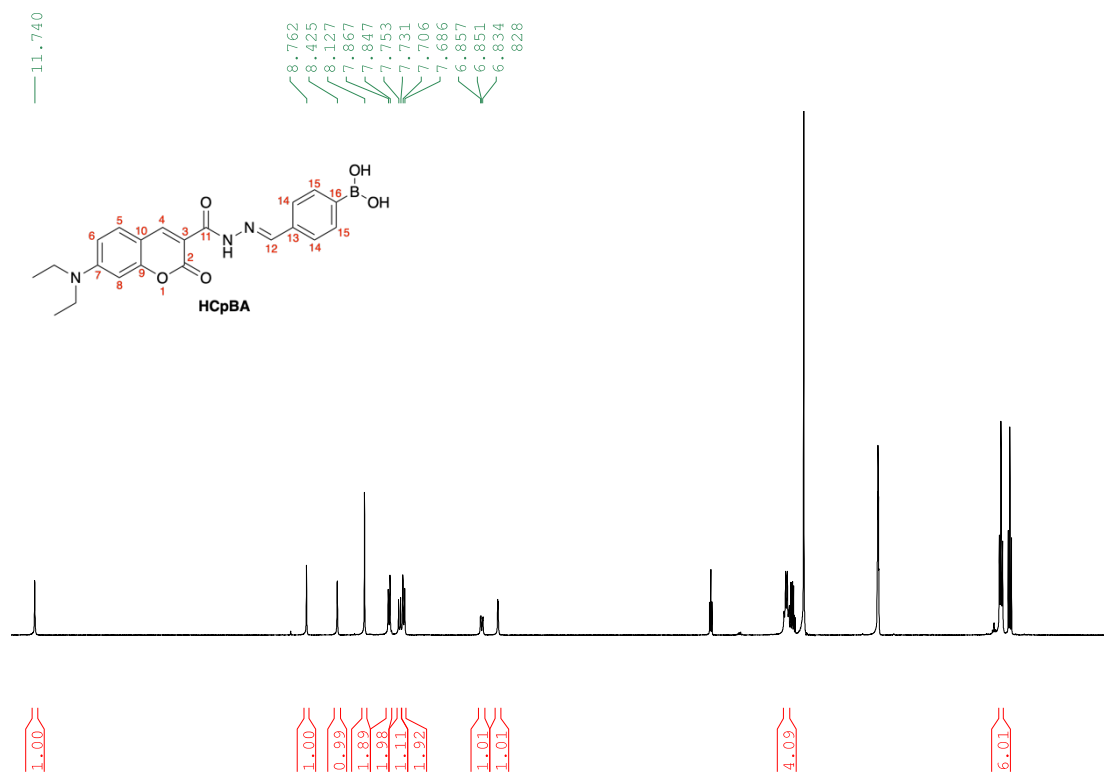


Figure S9.1: ^1H NMR spectrum of **HCpBA** in $\text{DMSO}-d_6$.

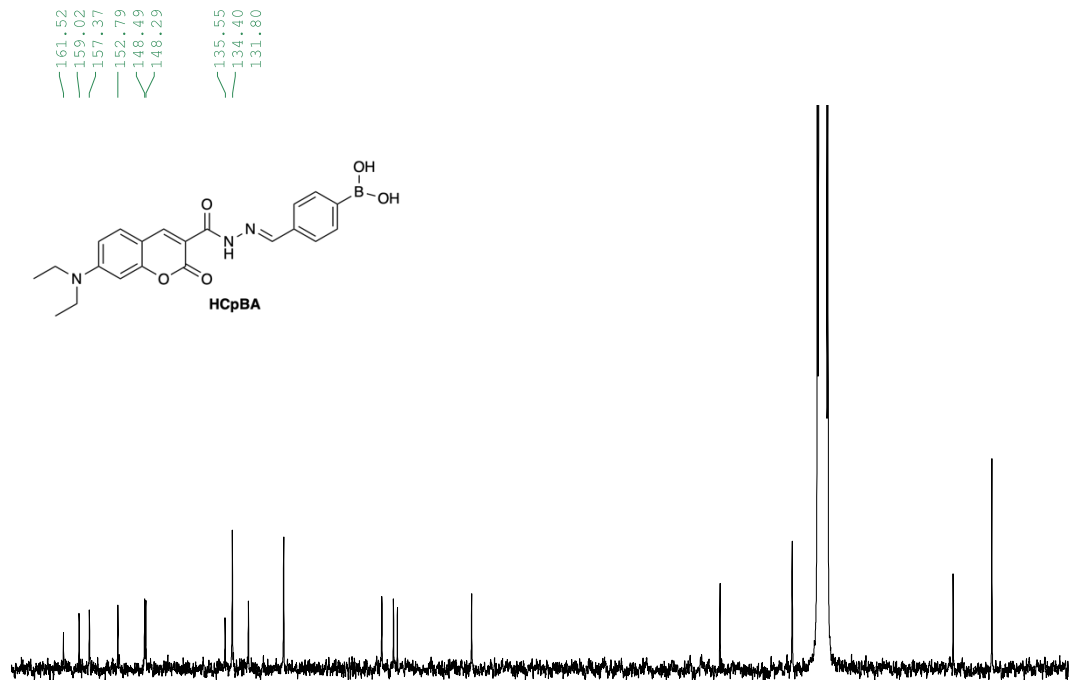


Figure S9.2: ^{13}C NMR spectrum of HCpBA in $\text{DMSO}-d_6$.

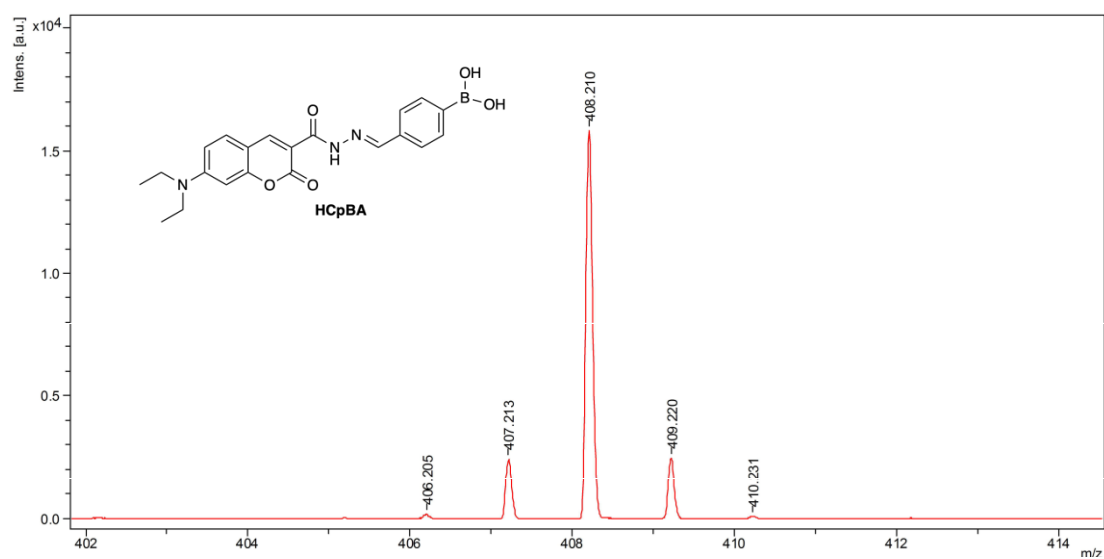


Figure S9.3: MALDI-TOF mass spectrum of **HCpBA**.

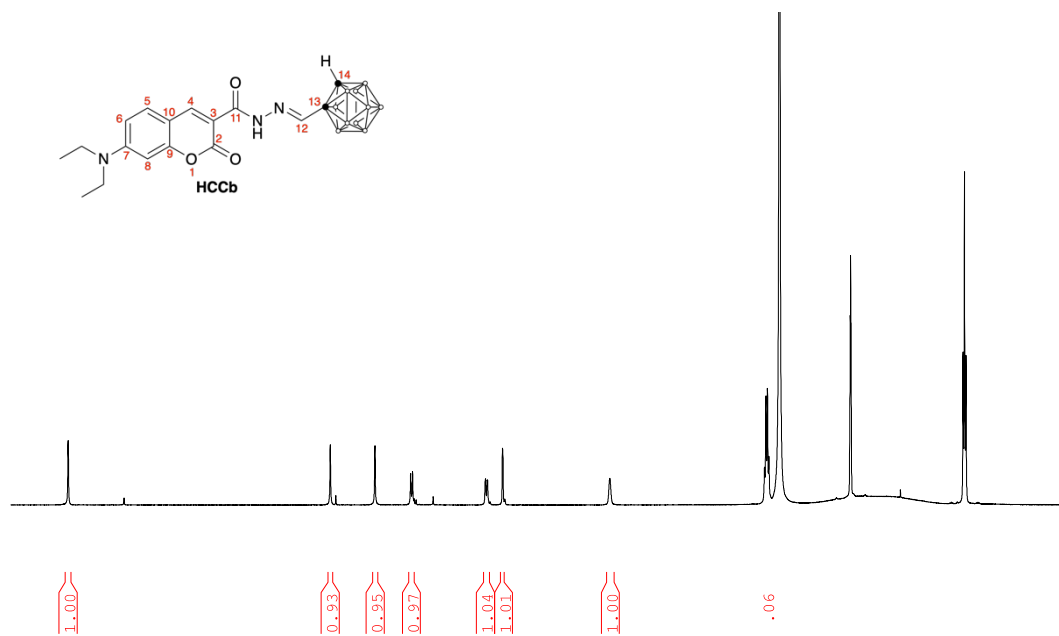


Figure S10.1: ¹H NMR spectrum of **HCCb** in DMSO-*d*₆

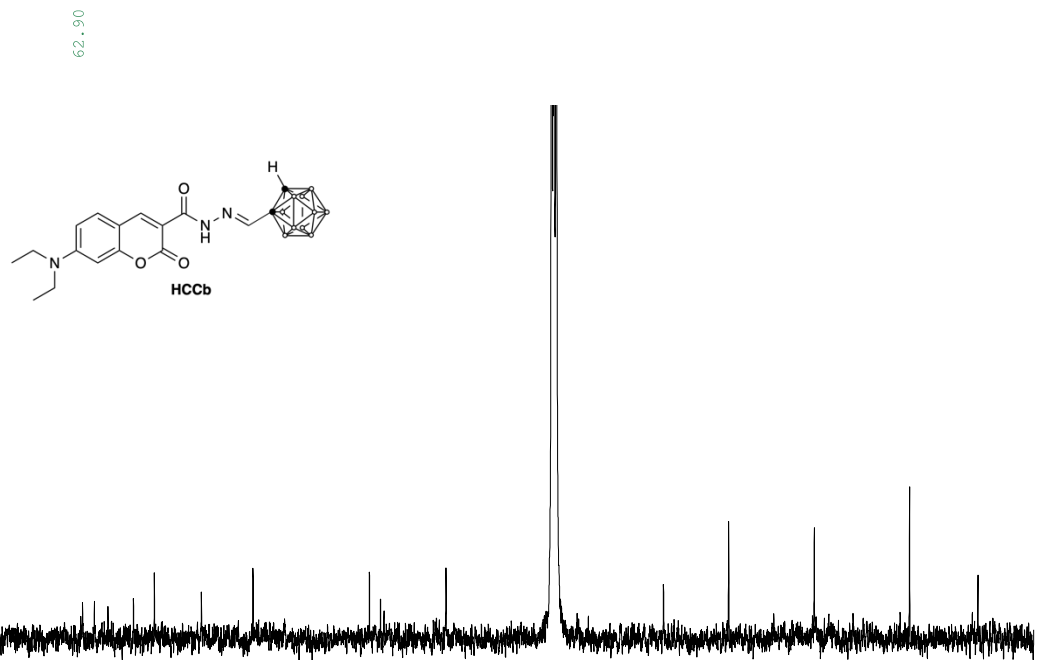


Figure S10.2: ^{13}C NMR spectrum of **HCCb** in CDCl_3 .

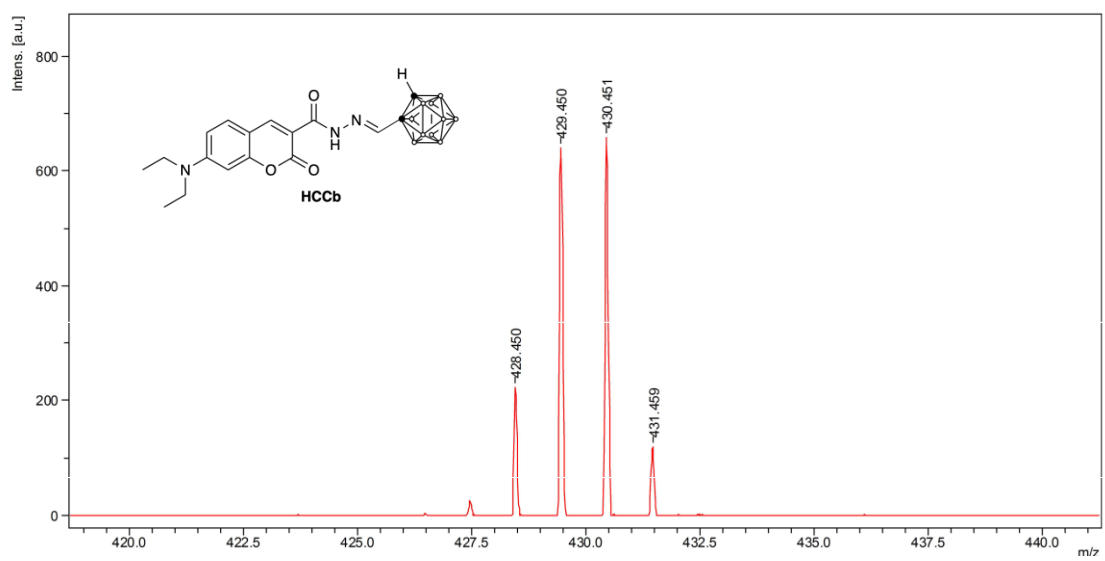


Figure S10.3: MALDI-TOF mass spectrum of **HCCb**.

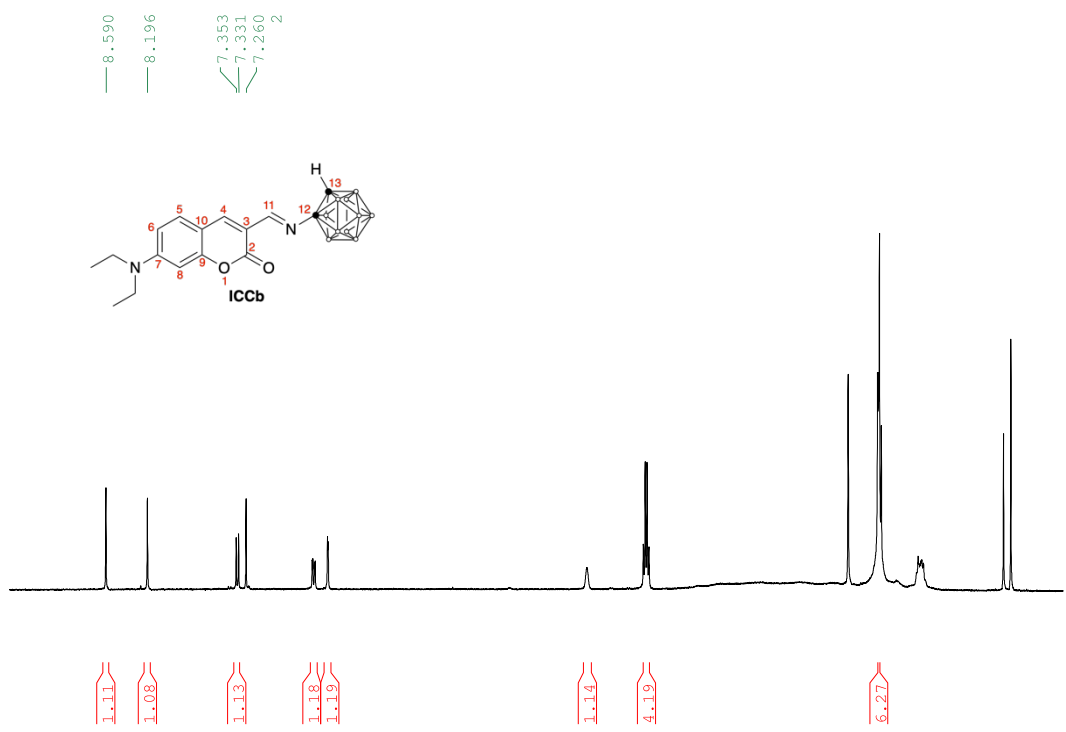


Figure S11.1: ^1H NMR spectrum of **ICCb** in CDCl_3 .

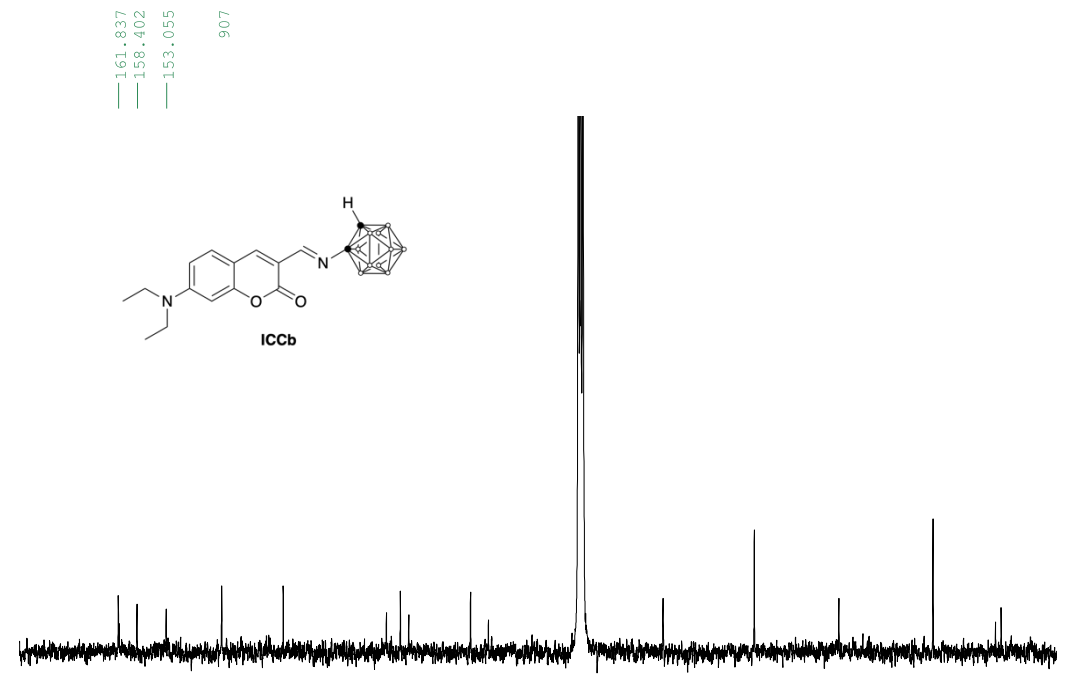


Figure S11.2: ^{13}C NMR spectrum of **ICCb** in CDCl_3 .

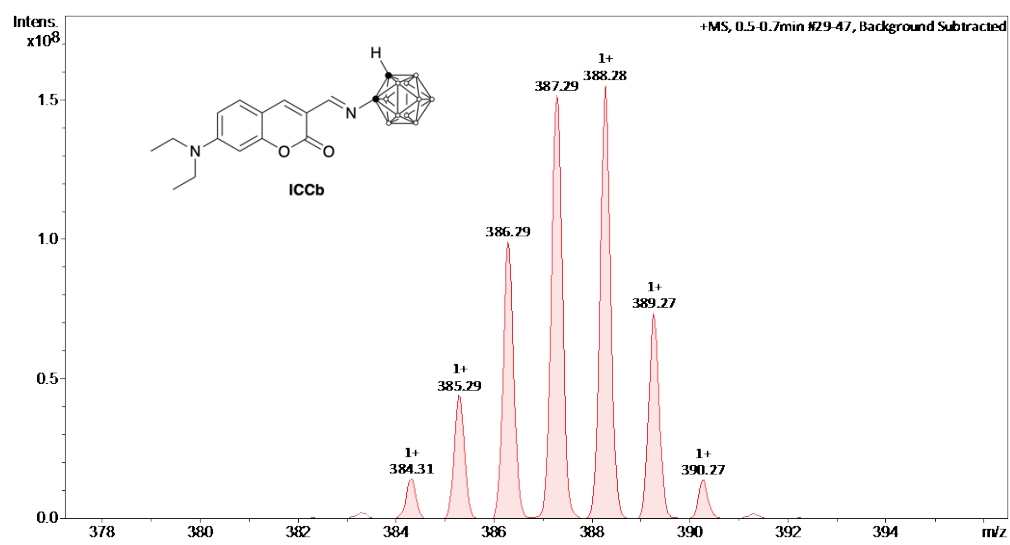


Figure S11.3: APCI mass spectrum of **ICCb**.